Supplemental Data

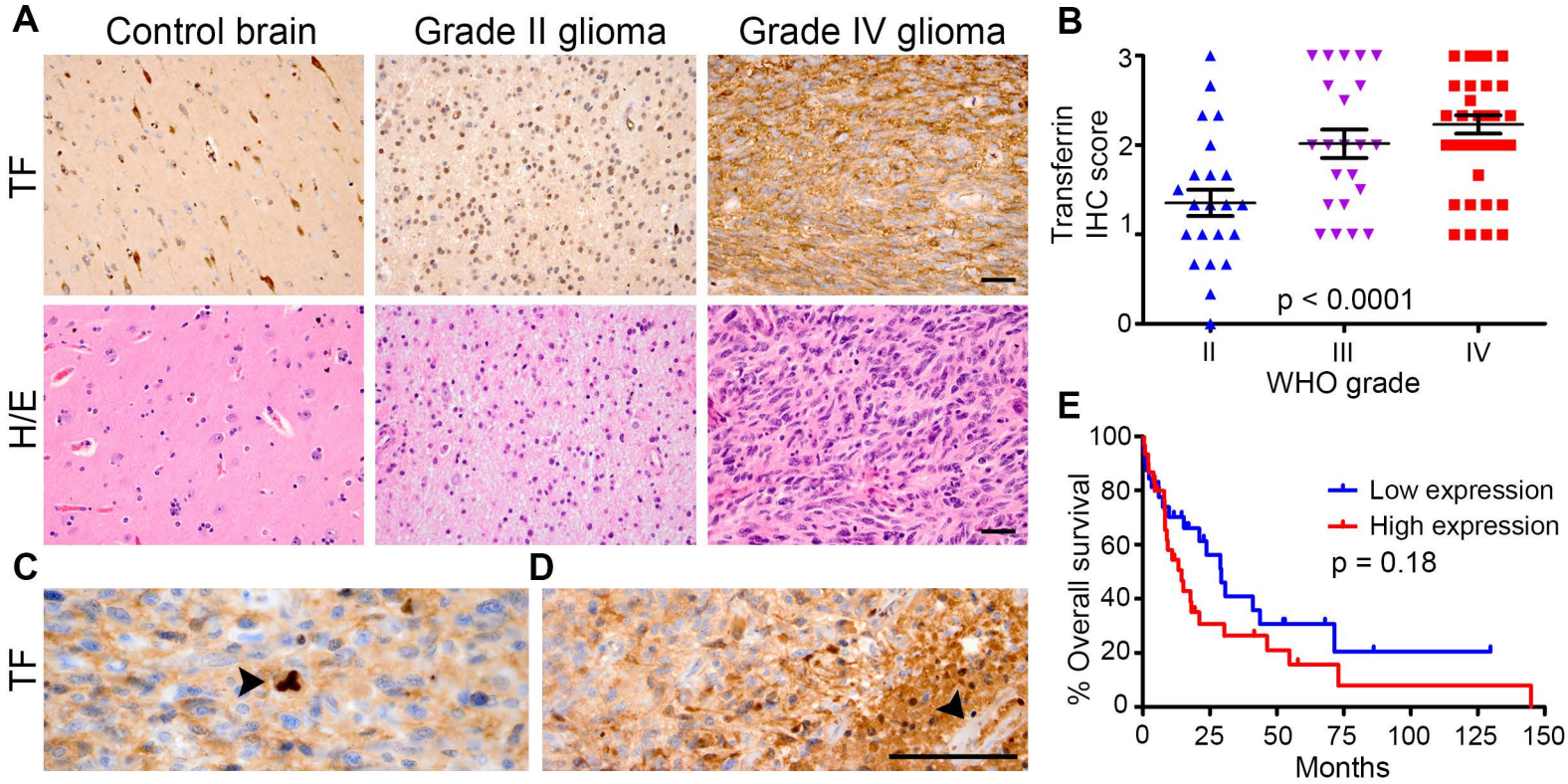

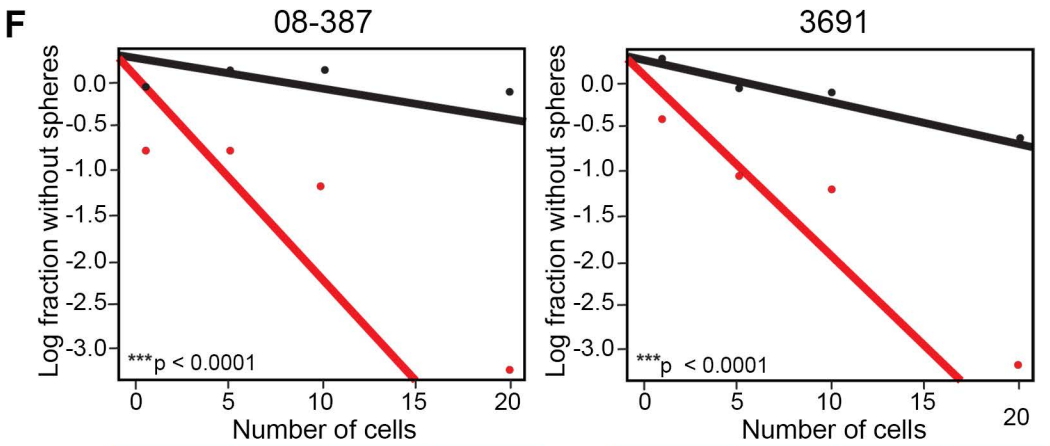

Stem Cell Frequency	Lower	Estimate	Upper
CD133⁻	70.7	41.2	24.1
CD133⁺	6.4	4.7	3.4

Stem Cell Frequency	Lower	Estimate	Upper
CD133⁻	54.9	32.9	19.7
CD133⁺	7.1	5.2	3.8

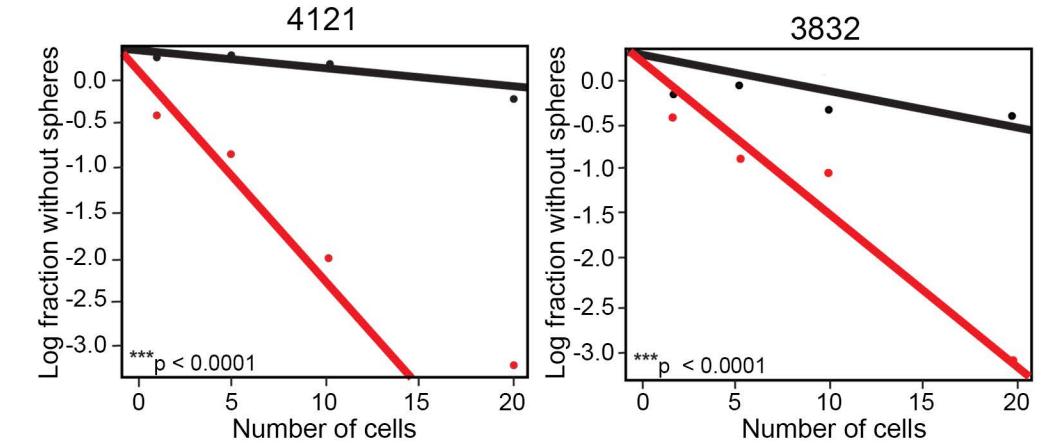

Stem Cell Frequency	Lower	Estimate	Upper
CD133⁻	143.1	71.3	35.5
CD133⁺	6.6	4.8	3.5

Stem Cell Frequency	Lower	Estimate	Upper
CD133⁻	71.6	44.2	27.3
CD133⁺	9.0	6.7	4.9

Figure S1, Related to Figure 1. TF expression is elevated in GBM. (A) TF immunohistochemistry of control brain, Grade II glioma and Grade IV glioma tissue – all of which were derived from the Horbinski tissue microarray (Top). Adjacent tissue sections were stained with H/E (Hematoxylin and Eosin) (Bottom). (B) Quantification of TF intensity with glioma grade. Error bars represent ± SEM. (C, D) TF immunohistochemistry in GBM tissue containing mitotic cells (C, see arrow) and perivascular regions (D, arrow denotes blood vessel). Scale bars = 50 μm. (E) Analysis of GBM patient survival based on TF expression. (F) Four freshly dissociated GBM xenografts were sorted via FACS for $CD133^{+}$ or $CD133^{-}$ in a limited dilution format (cell densities of 1, 5, 10, 20 cells per well), calculated with extreme limiting dilution assay (ELDA) analysis (Top). Y-axis represents log fraction of wells without spheres. Stem cell frequency confidence intervals were calculated as the ratio 1/x, where 1 = stem cell and x = all cells (Bottom).

Table S1, Related to Figure 1

Specimen information

Tumor Designation	Pathologic Histology	WHO Grade	Patient Age (Year)	Primary/ Recurrent	Chromosome 7	Chromosome 10	*PTEN*	*EGFR*	Percent $CD133^{+}$/ Total Population
3691	Glioblastoma	IV	58	Primary	77% Polysomy	54% Loss	49% Allelic Loss	WT 83% of cells positive for Polysomy	8.23
3832	Glioblastoma	IV	75	Primary	82% Polysomy	70% Loss	73% Allelic Loss	WT 97% of cells have amplified EGFR locus (20% of cells Positive for EGFRvIII)	1.54
08-387	Glioblastoma	IV	76	Primary	76% Polysomy	36% Loss	50% Allelic Loss	WT	2.52
4121	Anaplastic Astrocytoma	III	26	Recurrent	78% Polysomy	Intact	79% Polysomy	WT 48% of cells have loss of EGFR locus	7.37
GBM10	Glioblastoma	IV	41	Recurrent	N/A	N/A	Null	WT	4.34
GBM12	Glioblastoma	IV	68	Primary	N/A	N/A	WT	WT Amplified	10.35

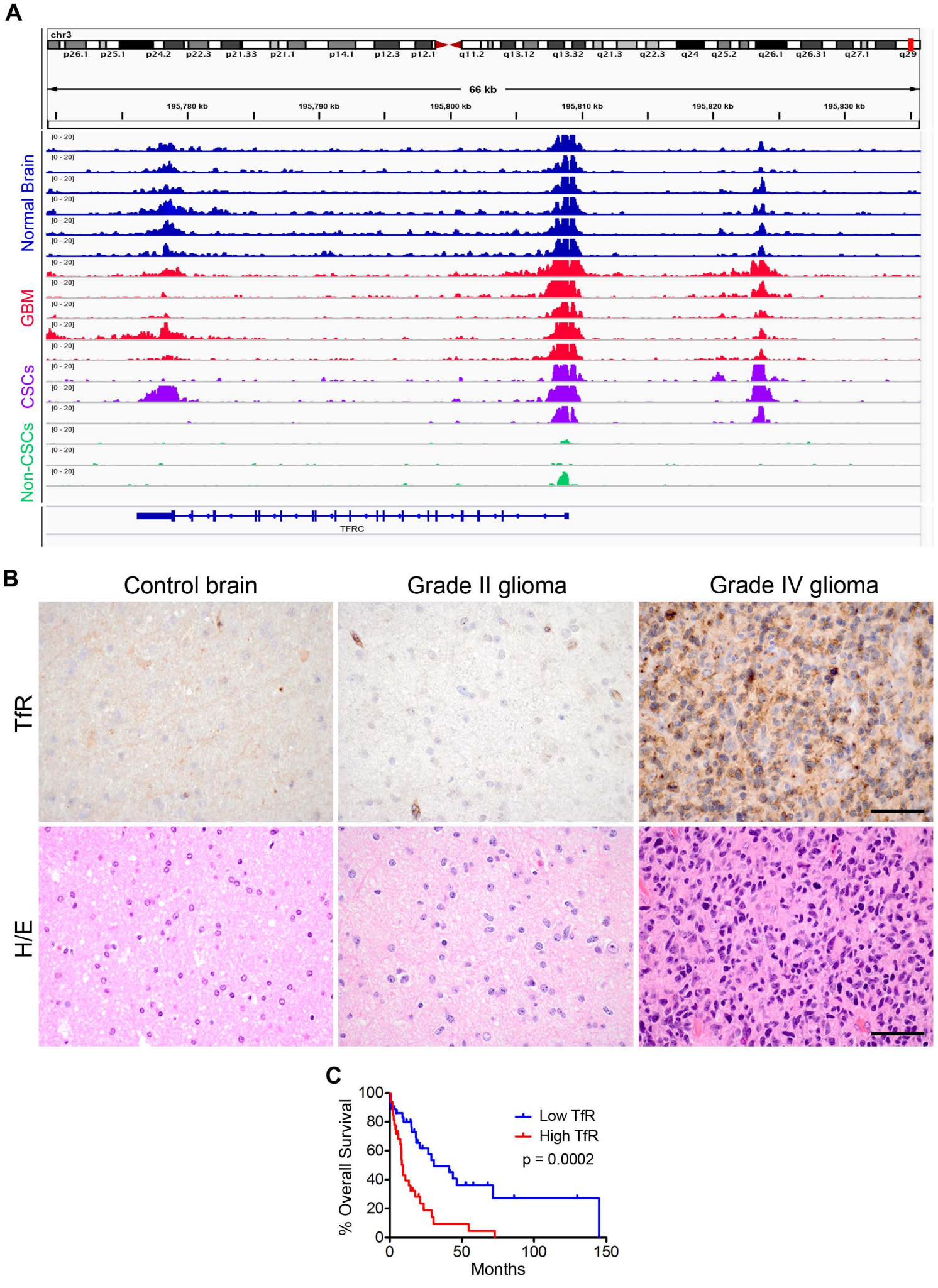
A
chr3
p26.1 p25.1 p24.2 p22.3 p21.33 p21.1 p14.1 p12.3 p12.1 q11.2 q13.12 q13.32 q21.3 q22.3 q24 q25.2 q26.1 q26.31 q27.1 q29
66 kb
195,780 kb
195,790 kb
195,800 kb
195,810 kb
195,820 kb
195,830 kb
Normal Brain
GBM
CSCs
Non-CSCs
[0 - 20]
TFRC
B
Control brain
Grade II glioma
Grade IV glioma
TfR
H/E
C
% Overall Survival
Months
Low TfR
High TfR
p = 0.0002
0
20
40
60
80
100
0
50
100
150

Figure S2, Related to Figure 2. Transferrin receptor (TfR) expression is increased in high-grade glioma patient tissue sections. (A) H3K27ac ChIP-seq enrichment plot centered at the *TFRC* locus. Enrichment is shown for various normal brain regions (Blue, Roadmap Epigenomics Project), a series of five primary GBMs (Red), GBM CSCs (Purple, n=3, (Suvà et al., 2014), and differentiated GBM cells (Green, n=3). (B) TfR immunohistochemistry of control brain, Grade II glioma, and Grade IV glioma tissue – all of which were derived from the Horbinski tissue microarray (Top). Adjacent tissue sections were stained with H/E (Hematoxylin and Eosin) (Bottom). Scale bars = 100 μm. (C) Correlation of TfR protein expression with patient survival (data derived from the Horbinski TMA).

A

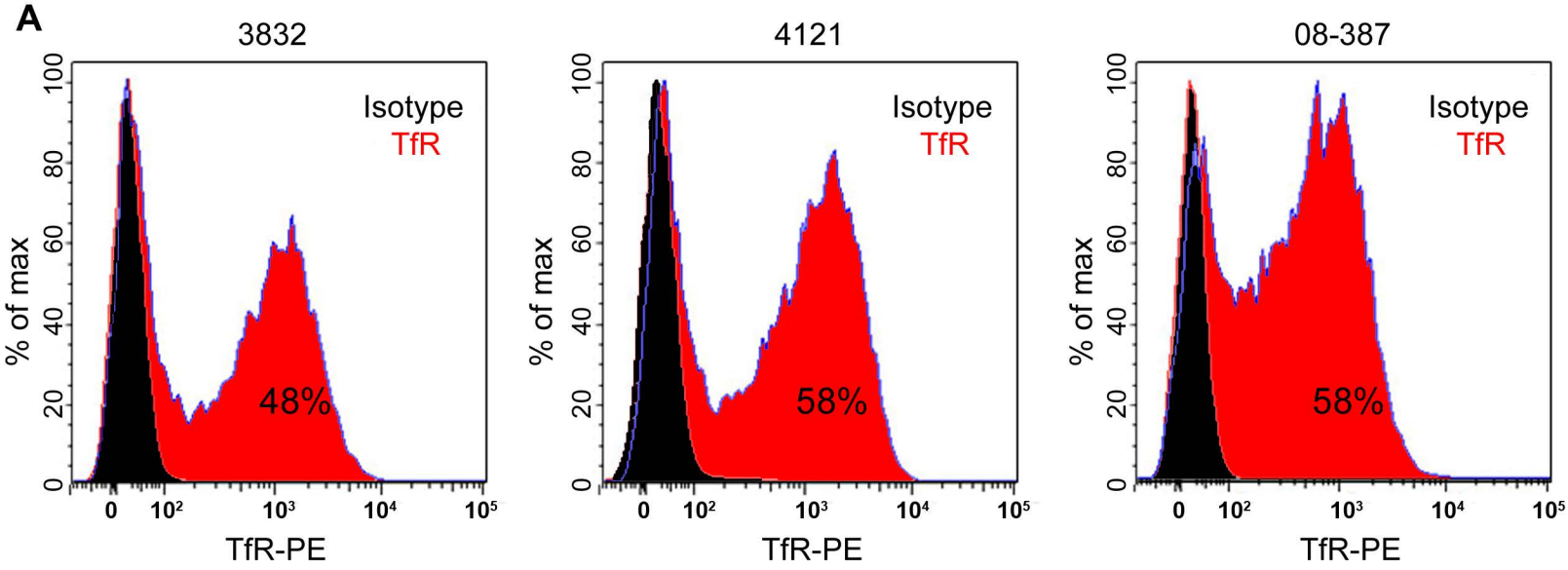

B

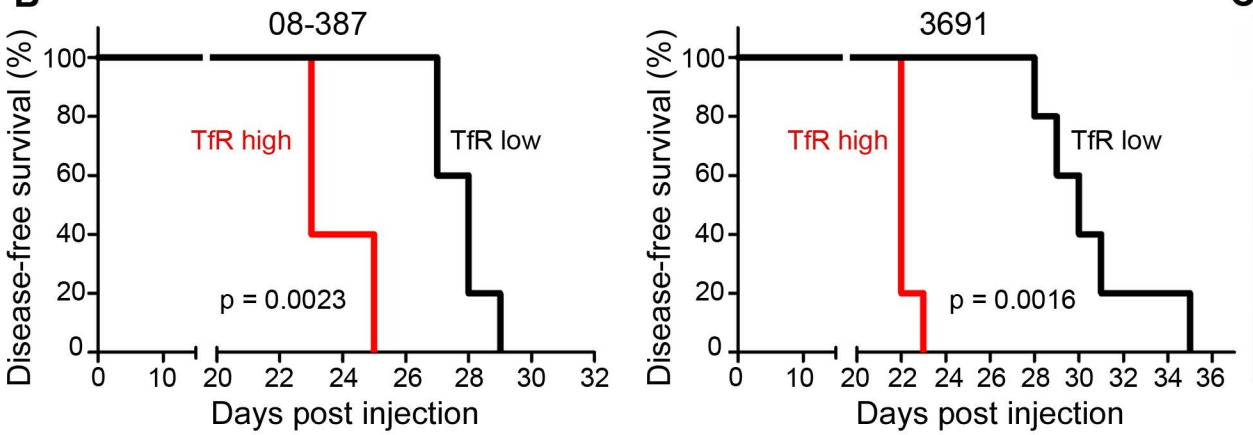

C

In vivo 10,000 cells	Median survival (days)
08-387 TfR High	23
08-387 TfR Low	28
3691 TfR High	22
3691 TfR Low	30

D

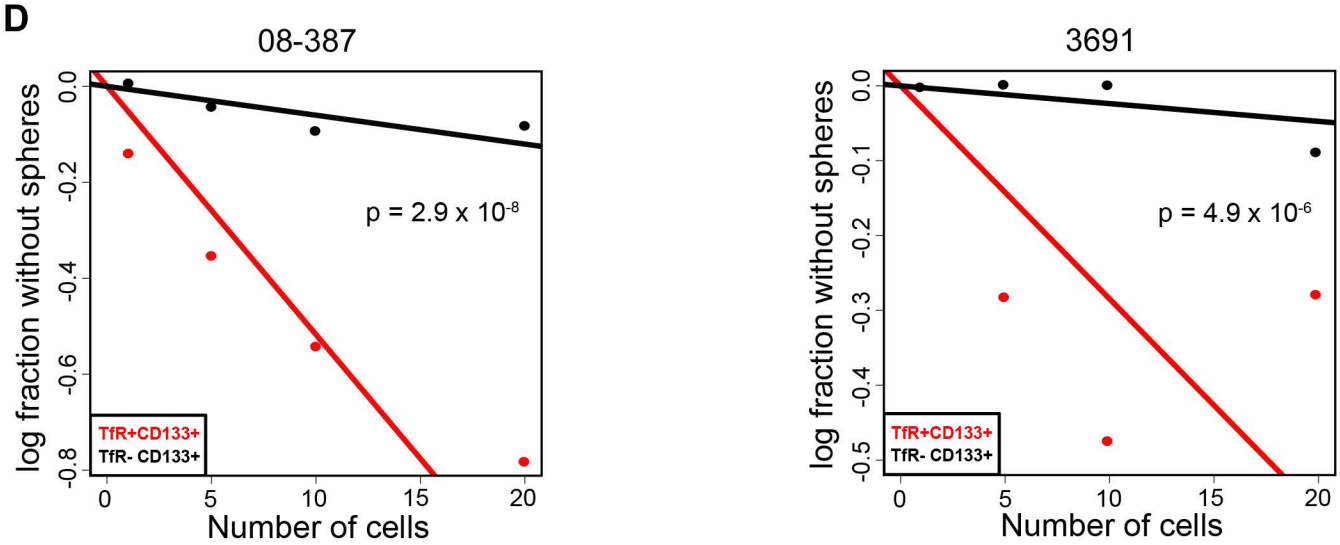

E

08-387

Stem Cell Frequency	Lower	Estimate	Upper
TfR⁺ CD133⁺	28	19	14
TfR⁻ CD133⁺	400	166	69

3691

Stem Cell Frequency	Lower	Estimate	Upper
TfR⁺ CD133⁺	69	43	27
TfR⁻ CD133⁺	1680	422	106

Figure S3, Related to Figure 3. GBM xenografts contain a significant population of TfR-positive cells, which predict tumor formation in vivo. (A) Three different GBM specimens were sorted using flow cytometry with a TfR-PE antibody (BD Biosciences). Expression was compared to isotype control. (B) Kaplan-Meier survival curves (in days) from mice intracranially injected with 10,000 cells derived from freshly dissociated GBM specimens sorted for TfR high (top 20% of cells expressing TfR) or TfR low (bottom 20% of cells expressing TfR) (n = 5/group). (C) Median survival (in days) of mice orthotopically injected with TfR-high or TfR-low expressing GBM cells. (D) GBM xenograft 08-387 and 3691 were sorted for $CD133^+$ with TfR (red) or without TfR (black) expression in a limited dilution format (cell densities of 1, 5, 10, 20 cells per well). Y-axis represents log fraction of wells without spheres. (E) Stem cell frequency confidence intervals were calculated as the ratio 1/x, where 1 = stem cell and x = all cells.

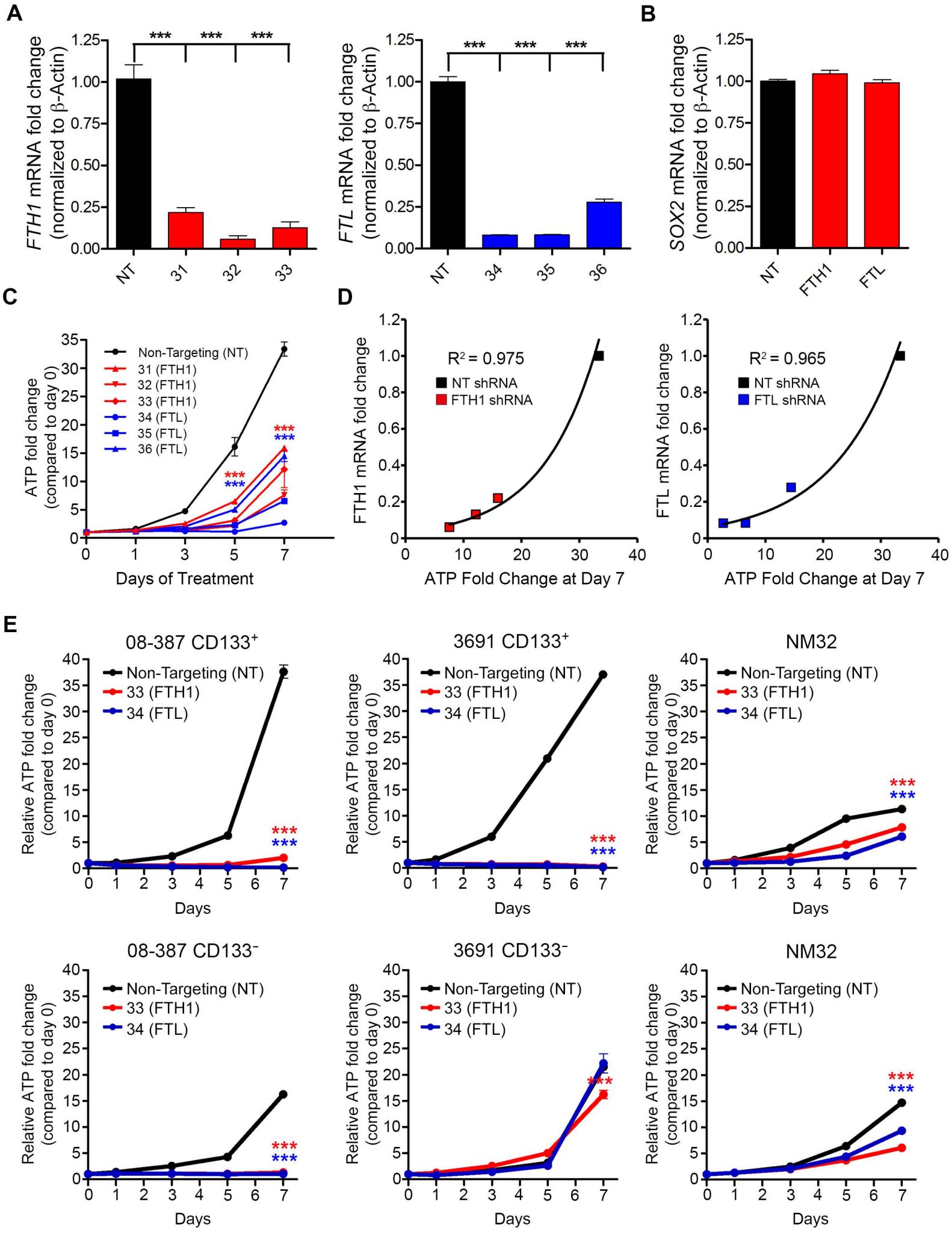
A
FTH1 mRNA fold change (normalized to β-Actin)
***
NT
31
32
33
FTL mRNA fold change (normalized to β-Actin)
NT
34
35
36
B
SOX2 mRNA fold change (normalized to β-Actin)
NT
FTH1
FTL
C
ATP fold change (compared to day 0)
Non-Targeting (NT)
31 (FTH1)
32 (FTH1)
33 (FTH1)
34 (FTL)
35 (FTL)
36 (FTL)
Days of Treatment
D
FTH1 mRNA fold change
R² = 0.975
NT shRNA
FTH1 shRNA
ATP Fold Change at Day 7
FTL mRNA fold change
R² = 0.965
NT shRNA
FTL shRNA
ATP Fold Change at Day 7
E
08-387 CD133+
3691 CD133+
NM32
08-387 CD133-
3691 CD133-
NM32
Relative ATP fold change (compared to day 0)
Non-Targeting (NT)
33 (FTH1)
34 (FTL)
Days

Figure S4, Related to Figure 5. (A) RT-PCR of *FTH1* or *FTL* mRNA expression in CSCs (from specimen 08-387) transduced with multiple FTH1 (31, 32, 33*) and FTL (34*, 35, 36) shRNA constructs. * denotes construct used throughout manuscript. (B) To demonstrate no off-target effects from ferritin knockdown, RT-PCR of *SOX2* expression following transduction of NT, FTH1 (construct 33), or FTL (construct 34) shRNAs. (C) Growth curve of 08-387 CSCs transduced with multiple FTH1 or FTL shRNA constructs. Cell growth was assessed by ATP CellTiter-Glo® Luminescent Cell Viability Assay. One-way ANOVA was used for comparing respective growth changes due to ferritin knockdown. ***, $p < 0.001$. (D) Knockdown/ATP ratio curves (along with R^2 values) demonstrate the correlation between FTH1 or FTL knockdown level and fold change in ATP (growth). (E) CSCs and non-CSCs from GBM xenografts 08-387 and 3691 and non-neoplastic human brain cells from specimens NM32 and NM34 were transduced with either non-targeting (NT), FTH1 (construct 33), or FTL (construct 34) shRNA, puro-selected at 48 hr and plated (in triplicates) in NBM medium plus supplements with 1% FBS. Cell growth was assessed by ATP CellTiter-Glo® Luminescent Cell Viability Assay. Two-way ANOVA was used for comparing respective growth changes due to ferritin knockdown within each cell type, *** , $p < 0.001$. Error bars represent ± SEM.

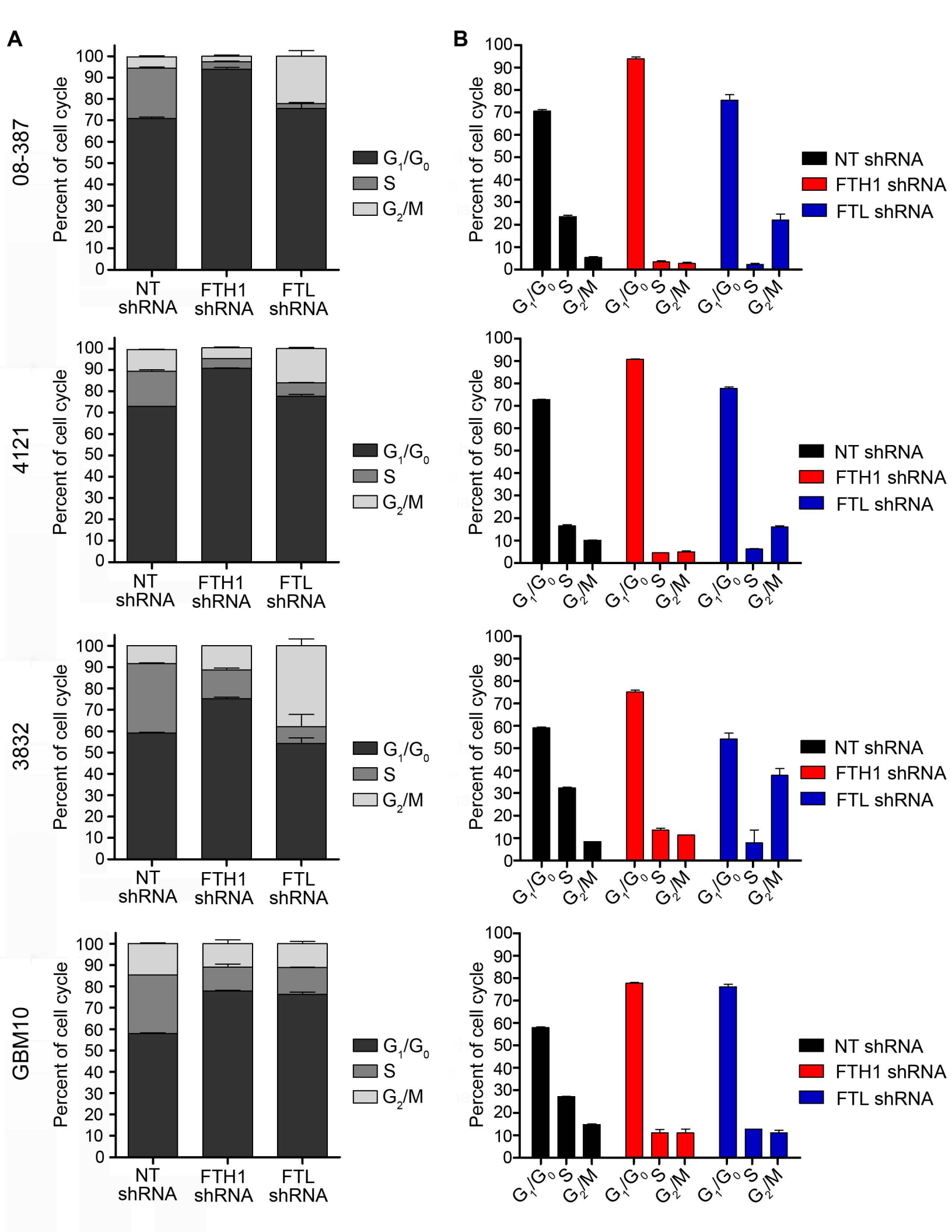
A
B
08-387
4121
3832
GBM10
Percent of cell cycle
NT shRNA
FTH1 shRNA
FTL shRNA
G1/G0
S
G2/M

Figure S5, Related to Figure 6. Ferritin knockdown alters the CSC cell cycle. (A) Cell cycle analysis demonstrated by a single vertical bar representing the entire cycle for each specimen and respective treatment (non-targeting (NT), FTH1, or FTL shRNA). (B) Each phase of the cell cycle is represented by a separate bar with non-targeting (NT) shRNA in black, FTH1 shRNA in red, and FTL shRNA in blue. Error bars represent ± SEM.

Table S2, Related to Figure 6

Gene	Aliases	FTH1 Fold Change	FTL Fold Change
ARHGAP1	Rho GTPase Activating Protein 1	-2.100097445	-2.073547639
ARHGAP11A	Rho GTPase Activating Protein 11A	-3.006147626	-2.442952257
ARHGAP11B	Rho GTPase Activating Protein 11B	-2.786042613	-2.340275479
ASF1B	Anti-Silencing Function 1B Histone Chaperone	-2.357132454	-2.089080103
ASNS	Asparagine Synthetase (Glutamine-Hydrolyzing)	-2.482198734	-2.314782442
ASPM	Abnormal Spindle Homolog, Microcephaly Associated	-3.436808438	-2.505625548
ATAD2	ATPase Family, AAA Domain Containing 2	-2.725833758	-2.386384736
ATAD5	ATPase Family, AAA Domain Containing 5	-2.854323286	-2.265365187
BIRC5	Baculoviral IAP Repeat Containing 5	-3.163051218	-2.130209416
BLM	Bloom Syndrome Protein	-2.819138297	-2.272675736
BRIP1	BRCA1 Interacting Protein C-Terminal Helicase 1	-2.741681869	-2.401346236
BUB1	BUB1 Mitotic Checkpoint Serine/Threonine Kinase	-3.160946177	-2.35465002
BUB1B	BUB1 Mitotic Checkpoint Serine/Threonine Kinase B	-2.935592581	-2.144211106
C4orf46	Chromosome 4 Open Reading Frame 46	-3.156113038	-2.171937174
CASC5	Cancer Susceptibility Candidate 5	-2.98304119	-2.242471815
CASP2	Caspase 2, Apoptosis-Related Cysteine Peptidase	-2.25830875	-2.838953802
CCNA2	Cyclin A2	-2.99036128	-2.247326267
CCNB1	Cyclin B1	-2.132930507	-2.252483485
CCNB2	Cyclin B2	-2.332469843	-2.458196801
CCNE2	Cyclin E2	-2.120703636	-2.755118622
CDC6	Cell Division Cycle 6	-3.656062658	-2.308511856
CDCA2	Cell Division Cycle Associated 2	-2.563109516	-2.289192896
CDCA8	Cell Division Cycle Associated 8	-3.350550345	-5.194925591
CDK1	Cyclin-Dependent Kinase 1	-4.008728404	-2.202521607
CENPE	Centromere Protein E	-3.374580397	-2.739784003
CENPF	Centromere Protein F	-2.627743781	-2.281986875
CENPH	Centromere Protein H	-2.269414174	-2.565845056
CENPI	Centromere Protein I	-3.0878974	-2.169949724
CENPK	Centromere Protein K	-2.481409729	-2.007007389
CHAF1B	Chromatin Assembly Factor 1 Subunit B	-2.011915314	-2.040538472
CIT	Citron (Rho-interacting, Serine/Threonine Kinase 21)	-2.602831908	-2.085702793
CKAP2L	Cytoskeleton Associated Protein 2-Like	-3.184352568	-2.200043563
CSNK1G1	Casein Kinase 1, Gamma 1	-2.831506554	-2.466257982
DEPDC1B	DEP Domain Containing 1B	-2.324182465	-3.042281758
DLGAP5	Discs, Large Homolog-Associated Protein 5	-4.732604752	-2.190138489
DNA2	DNA Replication Helicase/Nuclease 2	-1.996605911	-2.127545414
DSCC1	DNA Replication and Sister Chromatid Cohesion 1	-2.627978658	-2.170616173
DTL	Denticleless E3 Ubiquitin Protein Ligase Homolog	-5.207303663	-3.048622328
E2F1	E2F Transcription Factor 1	-3.03664415	-2.437934283
EME1	Essential Meiotic Structure-Specific Endonuclease 1	-2.693578605	-2.944335806

EXO1	Exonuclease 1	-3.538048384	-2.700138694
FAM72C	Family with Sequence Similarity 72, Member C	-2.376159846	-3.177571805
FAM72D	Family with Sequence Similarity 72, Member D	-2.869025039	-4.520752089
FAM83D	Family with Sequence Similarity 83, Member D	-2.419538765	-3.661211797
FANCA	Fanconi Anemia Complementation Group A	-2.369437285	-2.083273302
FANCD2	Fanconi Anemia Complementation Group D2	-2.831952192	-2.899021225
FANCI	Fanconi Anemia Complementation Group D1	-3.055467782	-2.421838057
FOXM1	Forkhead Box M1	-2.252518113	-2.337961689
GINS1	GINS Complex Subunit 1	-3.668620776	-2.882010843
GINS4	GINS Complex Subunit 4	-2.591182007	-2.267764774
GTSE1	G2 and S Phase Expressed 1	-2.341113872	-2.46911161
H2AFX	H2A Histone Family Member X	-2.232270879	-2.183272519
HIST1H1B	Histone Cluster 1, H2bm	-4.648952288	-4.761816593
HIST1H2BM	Histone Cluster 1, H2bm	-2.886196981	-3.641032605
HIST1H3A	Histone Cluster 1, H3a	-2.791068215	-3.422134358
IQGAP3	IQ Motif Containing GTPase Activating Protein 3	-3.042187435	-2.683726921
KIAA0101	Hepatitis C Virus NS5A-Transactivated Protein 9	-2.026266516	-2.268715759
KIAA1524	Cancerous Inhibitor of PP2A	-2.446406529	-2.173773317
KIF11	Kinesin Family Member 11	-2.563172908	-2.07112778
KIF14	Kinesin Family Member 14	-4.040167754	-2.463924568
KIF15	Kinesin Family Member 15	-3.366250747	-2.375086063
KIF18B	Kinesin Family Member 18B	-4.169723566	-2.52191692
KIF23	Kinesin Family Member 23	-2.5116134	-2.585619253
KIF24	Kinesin Family Member 24	-3.412765605	-2.181143533
KIF2C	Kinesin Family Member 2C	-2.522854936	-2.061550846
KIF4A	Kinesin Family Member 4A	-2.809228546	-2.572714602
*LRRC8B**	Leucine Rich Repeat Containing 8 Family, Member B	-2.148784742	-2.616046615
MAD2L1	MAD2 Mitotic Arrest Deficient-Like 1	-4.424990821	-3.663226718
MCM10	Minichromosome Maintenance Complex Component 10	-4.313448696	-2.291378484
MELK	Maternal Embryonic Leucine Zipper Kinase	-2.340616811	-2.62353443
mir-153	microRNA 153	-2.23556762	-2.211009742
MKI67	Proliferation-Related Ki67 Antigen	-3.328446635	-2.331253502
MLF1IP	MLF1 Interacting Protein	-2.47623887	-2.366237873
MND1	Meiotic Nuclear Divisions 1 Homolog	-2.988761477	-2.982586967
MYBL2	Myb related protein	-3.269891278	-2.02310389
NCAPG	Non-SMC Condensin 1 Complex Subunit G	-3.225581637	-2.160100196
NCAPH	Non-SMC Condensin 1 Complex Subunit H	-3.50431655	-3.981393744
NDC80	NDC80 Kinetochore Complex Component	-2.478015127	-4.689359052
NOP56	NOP56 Ribonucleoprotein	-2.031750229	-2.170476648
NUSAP1	Nucleolar and Spindle Associated Protein 1	-3.06601978	-2.047744735
OIP5	Opa Interacting Protein 5	-2.43630853	-2.471162298
ORC1	Origin Recognition Complex Subunit 1	-2.475792017	-2.157975965
ORC6	Origin Recognition Complex Subunit 6	-3.222101272	-2.107760865
PBK	PDZ Binding Kinase	-3.402528775	-2.076981572

PLK1	Polo-Like Kinase 1	-3.157806409	-2.307262722
PLK4	Polo-Like Kinase 4	-3.978470068	-3.012893406
POLQ	Polymerase (DNA Directed) Theta	-4.08005275	-2.160681618
PPIF	Peptidylprolyl Isomerase F	-2.507860271	-3.560698453
PRC1	Protein Regulator of Cytokinesis 1	-2.932580233	-2.297622682
PRR11	Proline Rich 11	-2.603400115	-2.584430477
PTBP1	Polypyrimidine Tract Binding Protein 1	-2.527872921	-2.070253288
RAD51AP1	RAD51 Associated Protein 1	-2.833281324	-2.113626635
RAD54L	RAD54-Like	-3.190345053	-2.210399262
RNASEH2A	Ribonuclease H2 Subunit A	-2.486325155	-2.04579767
RPS8	Ribosomal Protein S8	-2.118464381	-2.169068305
RRM2	Ribonucleotide Reductase M2	-2.563334772	-2.8966336
SEH1L	Nucleoporin Seh1	-2.617230249	-2.204340804
SGOL1	Shugoshin-Like 1	-3.904129153	-2.563014051
SKA1	Spindle and Kinetochore Associated Complex Subunit 1	-3.832725853	-5.06317026
SKA3	Spindle and Kinetochore Associated Complex Subunit 3	-3.41832225	-2.220197071
SLC39A3	Solute Carrier Family 39 Member 3	-2.027805223	-2.152113745
SNHG1	Small Nucleolar RNA , Host Gene 1	-2.10203371	-3.137994071
SNORD20	Small Nucleolar RNA , C/D Box 20	-2.073556504	-2.171920937
SPC25	NDC80 Kinetochore Complex Component	-3.517604075	-2.693890207
STARD7	Star-related Lipid Transfer Domain Containing 7	-3.580894142	-2.000565021
TICRR	TOPBP1-interacting Checkpoint and Replication Regulator	-3.659016154	-2.014088544
TK1	Thymidine Kinase 1	-3.014377641	-2.144968042
TMEM38B	Transmembrane Protein 38B	-2.327779527	-2.902612703
TMPO	Thymopoietin	-2.092624132	-2.539633424
TOP2A	Topoisomerase 2 Alpha	-3.470339853	-2.040864964
UBE2C	Ubiquitin-Conjugating Enzyme E2C	-3.229820965	-2.353121016
XRCC2	X-Ray Repair Cross-Complementing Protein 2	-2.610835809	-2.222520661
ZNF678	Zinc Finger Protein 678	-2.058176834	-3.052498643
ZNF714	Zinc Finger Protein 714	-2.003640094	-2.30720111
ZNF724P	Zinc Finger Protein 724	-2.52440518	-2.7920919
ZNF730	Zinc Finger Protein 730	-3.322506637	-2.245890488

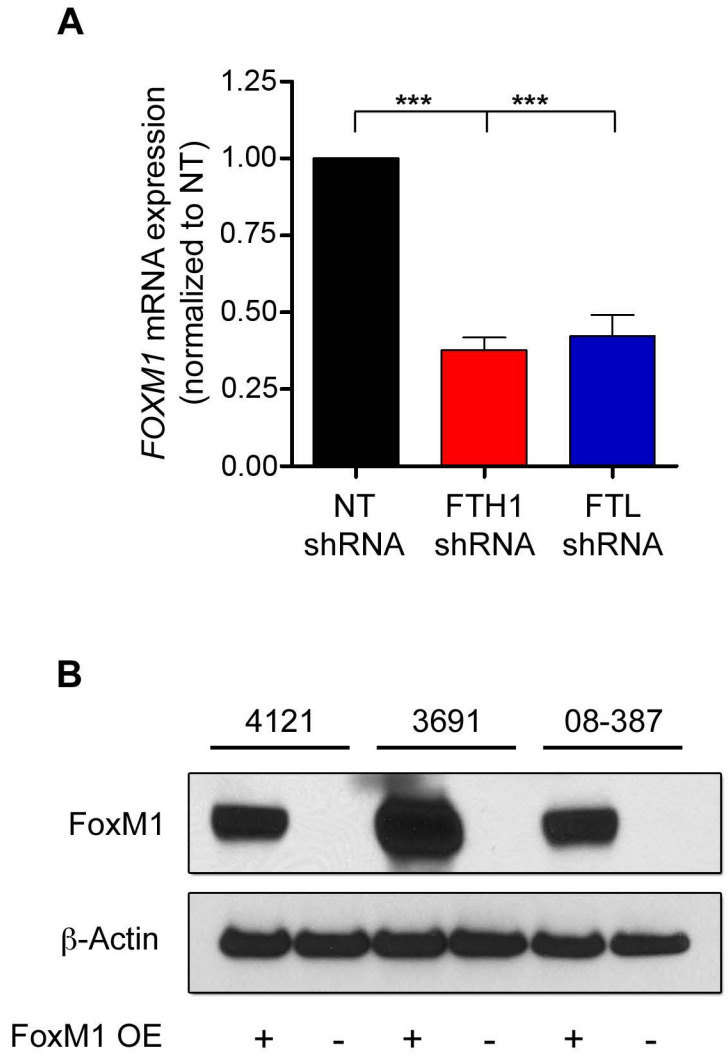

Figure S6, Related to Figure 7. Decreased *FOXM1* expression following ferritin knockdown. (A) Relative mRNA levels of *FOXM1* expression in CSCs with FTH1 or FTL shRNA compared to non-targeting (NT) control shRNA. Error bars were calculated by comparing expression from each specimen (with FTH1 or FTL shRNA), then normalized to matching NT shRNA CSCs. Data are represented as mean ± SEM. ***, $p < 0.001$. (B) FoxM1 overexpression was validated by Western blot in CSCs derived from three different GBM xenografts. β-Actin was used as a loading control.

Supplemental Experimental Procedures

Human GBM specimen culture conditions

Glioblastoma (GBM) tissues were obtained from excess surgical materials from patients with informed consent at Duke University, Mayo Clinic, Cleveland Clinic, University of Kentucky and Odense University Hospital after review from a neuropathologist in accordance with an approved protocol by the Institutional Review Board (USA) and the Committee on Health Research Ethics (Denmark). As previously described (Bao et al., 2006; Eyler et al., 2011; Flavahan et al., 2013; Hjelmeland et al., 2011; Lathia et al., 2010; Li et al., 2009b; Venere et al., 2014; Yan et al., 2014), GBM stem cells (CSCs) and/or non-CSCs were derived immediately after dissociation or after transient xenograft passage (fewer than five passages) in immunocompromised mice using prospective sorting either via magnetic columns (MACS, CD133 microbeads, Miltenyi Biotec) or flow cytometry (FACS, CD133/2-APC, Miltenyi Biotec) followed by functional analysis. The cancer stem cell phenotype of $CD133^+$ cells was confirmed by functional assays of stem cell marker expression, sphere formation by in vitro limiting dilution and secondary tumor initiation. CD133-negative cells did not share these properties and were used in matched assays as non-CSCs. For short-term in vitro expansion, CSCs were cultured in Neurobasal medium (NBM) with B27 (without vitamin A, Invitrogen), basic fibroblast growth factor (20ng/ml) and epidermal growth factor (20ng/ml), on Petri dishes. CD133-depleted non-CSCs were cultured in Dulbecco's modified Eagle medium (DMEM) with 10% FBS, on tissue-culture coated plates. For all experiments in which CSCs and non-CSCs were directly compared, Geltrex (Invitrogen) was used to attach cells to tissue-culture plates and a medium consisting of CSC medium with 1% FBS was used for long-term studies (beyond 24 hr) whereas in short-term experiments (less than 6 hr), a null medium consisting of only NBM was used.

hES-cell derived OPCs and isolation and culture of primary Normal Glial Progenitors

Derivation of human OPCs

Human OPCs were differentiated from the human embryonic stem cell line H7 over a 154 day protocol (NIH Human Embryonic Stem Cell Registry WA07; NIH Approval Number: NIHhESC-10-0061) as previously demonstrated (Hu et al., 2009; Wang et al., 2013). hESC-derived OPCs were characterized by co-staining of Sox10 (R&D Systems,AF2864; 1:100) and Olig2 (Millipore, AB9610 1:500).

Isolation of Normal Glial Progenitors

Normal (NM), non-neoplastic cells were derived from patient tissue specimens of neurosurgical resection in accordance with a Cleveland Clinic Institutional Review Board-approved protocol. Informed consent was obtained by the tissue bank, which provided de-identified excess tissue to the laboratory immediately following surgical resection. Specimens used for cell culture were dissociated with a Papain dissociation kit (Worthington). Cells were cultured adherently in media containing 50% Neurobasal medium (Gibco) and 50% Dulbecco's modified Eagle medium (DMEM) with B27 (without vitamin A, Invitrogen, basic fibroblast growth factor (10 ng/ml), epidermal growth factor (10 ng/ml), sodium pyruvate and L-glutamine, and 5% FBS. All cultured cells were used within five passages of dissociation**.**

Characterization of Normal Glial Progenitors

Single cells were sorted using anti-A2B5 MicroBeads (130-093-388, Miltenyi Biotec) according to manufacturer's protocol. In brief, live cells were incubated first with FcR Blocking Reagent (Miltenyi) for 10 min then A2B5 antibody for 15 min at 4oC (2.5 µg A2B5 antibody per million cells). Cells positive for A2B5 were double enriched by passing through magnetic field (MACS Separator) twice. Both A2B5 positive and negative fractions were collected, lysed with TRIzol (Invitrogen) for RNA isolation. A population of $A2B5^+$ cells were plated and allowed to attach overnight before fixing and staining with standard immunofluorescence techniques. $A2B5^+$ cells stained positive for GFAP (DAKO, 1:5000) and Nestin (DSHB, 1:200).

RNA-sequencing

RNA was extracted from ~2 x 10^6 cells with TRIzol (Invitrogen), separated using Phase Lock Gel tubes (5 Prime), and purified using the miRNAeasy kit (Qiagen) according to the manufacturer's protocol. PolyA+ RNA was prepared for sequencing using the Illumina TruSeq RNA Sample Preparation Kit according to the manufacturer's protocol. RNA-seq libraries were sequenced on the Illumina HiSeq 2500 platform at the Case Western Reserve University Genomics Core Facility. For gene expression analysis, reads were aligned to the hg19 genome build (retrieved from http://cufflinks.cbcb.umd.edu/igenomes.html), using Tophat v2.0.6 (Trapnell et al., 2009). The distribution of alignments was analyzed using the CollectRnaSeqMetrics module of Picard v1.89 (http://picard.sourceforge.net/). FPKM values for known genes were calculated using Cufflinks v2.0.2 (Trapnell et al., 2010) provided with the GTF file via the -G (known genes only) option. FPKM values were tabled by converting background values (<0.25) to 0 and adding 0.25 to all values (Ramsköld et al., 2009). Differential expression testing was performed using Cuffdiff v2.0.2; however, all FPKM values provided are those calculated by Cufflinks.

ChIP-sequencing

H3K4me1ChIP was performed from 5 x 10^6 crosslinked p0-CSCs and sequencing libraries were prepared as previously described (Rabbit anti-H3K4me1 Abcam #8895) (Corradin et al., 2014). ChIP-seq libraries were sequenced on the Illumina HiSeq 2500 platform at the Case Western Reserve University Genomics Core Facility. The FASTX-Toolkit (http://hannonlab.cshl.edu/fastx_toolkit/) was used to remove adapter sequences and trim read ends using a quality score cutoff of 20. ChIP-seq data were aligned to the hg19 genome assembly (retrieved from http://cufflinks.cbcb.umd.edu/igenomes.html), using Bowtie v0.12.9 (Langmead et al., 2009), allowing reads with ≤ 2 mismatches and discarding reads with > 1 reportable alignment ("-m 1" parameter). PCR duplicates were removed using SAMtools (Li et al., 2009a). Peaks were detected with MACS v1.4 (Zhang et al., 2008), using an aligned input

DNA sample as control. Wiggle tracks stepped at 25 bp were generated by MACS, normalized to the median signal by chromosome and visualized on the UCSC Genome Browser.

Geneset Enrichment Analysis

H3K27ac ChIP-seq enrichment plot centered at the *INSERT GENE* locus. Enrichment is shown for various normal brain regions (Blue, Roadmap Epigenomics Project), a series of five primary GBMs (Red), GBM stem cells (Purple, n=3, Suva et al., 2014), and differentiated GBM cells (Green, n=3). The Broad MsigDB databases: C2 canonical, REACTOME, and KEGG pathways were analyzed, along with custom genesets generated previously (Mack et al., 2014). Differences between NT shRNA, FTH1 shRNA, and FTL shRNA treatment groups were determined using the default GSEA: signal-to-noise ratio.

Prediction of gene targets of enhancer elements using PreSTIGE

Enhancer-gene assignments were made as described in (Corradin et al., 2014). Briefly, predictions were made using comparative analysis across a panel of 13 tissues. For an interaction to be predicted the normalized H3K4me1-enhancer signal intensity had to be above background and highly specific to the cell line of interest compared to the remaining 12 cell lines. Additionally, the gene must be within 100-kb of the enhancer and must show relatively cell type-specific transcript levels. PreSTIGE predictions for CSCs were made using independent comparisons to a panel that included bone marrow, cerebellum, embryonic heart, intestine, kidney, liver, lung, MEF, olfactory bulb, placenta, testis and thymus (selected for tissue diversity).

Tissue microarray immunohistochemistry and survival analysis

Briefly, de-identified tissue microarrays (TMAs) were constructed from gliomas after obtaining University of Kentucky Institutional Review Board Approval. Three 2-mm diameter cores per tumor were obtained, with each core embedded in a separate TMA block. A total of 104 cases

comprised the TMAs, including 9 nonneoplastic controls (cortical dysplasias), 9 grade II astrocytomas, 11 grade III astrocytomas, 12 anaplastic oligodendrogliomas, 16 grade II oligodendrogliomas, and 47 grade IV glioblastomas (GBMs). Each TMA core was semi-quantified on a relative scale from 0 to 3, with 0 = negative and 3 = strongest. Results from all 3 cores were averaged together to produce a final score for a tumor. Results were plotted based on WHO grade and differences were calculated via one-way ANOVA with post-hoc Tukey's test. Survival data was obtained on each case from the Kentucky Cancer Registry, and the degree of expression was correlated with survival via Log-rank (Mantel-Cox) Tests.

For immunohistochemistry, 5 μm TMA slides were baked at 60°C for 1 hr, followed by deparaffinization in xylene and stepwise hydration in alcohol to TBS-Tween. Endogenous peroxidases were quenched with 3% hydrogen peroxide for 5 min and antigen retrieval was performed with Dako's high pH antigen retrieval buffer by heating to 110°C for 20 min in a Biocare medical decloaking chamber followed by cooling to room temperature. Slides were blocked in 5% normal goat serum in TBST for 20 min and incubated in primary antibody for 1 hr at room temperature. Primary antibodies were as follows: Transferrin (TF, Sigma-Aldrich): 0.5 μg/mL in TBST, Transferrin Receptor (TfR, Invitrogen): 1μg/mL in TBST, Ferritin Heavy Chain (FTH1, Abcam): 0.5 μg/mL in TBST, Ferritin Light Chain (FTL, Abcam): 0.5 μg/mL in TBST. After washing in TBST, rabbit secondary antibody was applied for 30 min at room temperature (Dako Envision+ kit) followed by TBST washes and detection with DAB. Slides were then counterstained in Mayer's hematoxylin for 5 min and blued in ammonia water before dehydrating and cover slipping.

Ex vivo TF uptake imaging assay

CSCs and non-CSCs were labeled with Cell Tracker Red CMPTX and Cell Trace Far Red DDAO-SE, respectively (Invitrogen). Slice cultures were prepared from non-neoplastic mouse brains, according to prior publications (Stoppini et al., 1991). 100,000 cells total were

transplanted (at a ratio of 1:1) and incubated overnight to ensure integration and survival. 3 hr prior to imaging, slices were incubated in 50 µg/ml fluorescent-TF (Invitrogen). Imaging was done using a SP5 imaging system (Leica) with a 20x liquid immersion objective (numeric aperture of 1.0). Images were acquired at 820 nm and processed using Imaris software (Bitplane).

Iron uptake assay

As previously described (Sarkar et al., 2003), adherent CSCs and non-CSCs were incubated at 37°C with null NBM medium containing 10 µM ^{55}Fe-NTA ($^{55}FeCl_3$; Perkin Elmer), 90 µM Fe-NTA ($FeCl_3$; Sigma-Aldrich), and 100 µM ascorbate for 3 hr. After a PBS wash containing 100 µM EDTA to remove iron non-specifically bound to the cell surface, cells were washed two additional times with PBS, lysed with MP40, transferred to scintillation tubes and counted by liquid scintillation. To measure uptake of iron bound to transferrin (TF), similar procedures were performed as above except that ^{55}Fe-NTA was first conjugated to TF (Calbiochem) as previously described (Das et al., 2009).

Transferrin secretion assay

CSCs and non-CSCs from three xenograft specimens were plated and grown to equal confluency in identical medium conditions (see above). Medium was collected and concentrated using centrifugal filter with a 10K molecular weight cutoff. A BCA protein assay was then used to detect the total amount of protein within the media. 1µg protein from each cell line was added to a transferrin ELISA (Abcam Transferrin Human ELISA Kit)

Thymidine incorporation assay

Thymidine was added in a 4µl:46µl dilution of thymidine: neurobasal medium per well (100,000 cells/well in 12-well plate) and incubated for 4 hr at 37°C. Collected medium was spun at 1500 rpm for 5 min, washed repeatedly with cold PBS and once with cold 10% TCA. After 1 hr

incubation in 400µl cold 10% TCA, medium was incubated for 1 hr at 4°C, spun with pellet resuspended in 500µl of 0.2N NaOH. After incubation overnight at RT, medium was transferred to scintillation tubes and quantified using a scintillation counter.

Immunofluorescent staining

Cells or 10µm thick slides of xenografted brain tissue (n ≥ 3) were fixed in 4% paraformaldehyde and immunolabeled using the following antibodies: mouse anti-Transferrin Receptor (TfR/CD71, 1:250, Invitrogen), goat anti-Sox2 (1:500, R&D Systems), rabbit anti-Ferritin Light Chain (FTL, 1:250, Abcam), and rabbit anti-Ferritin Heavy Chain (FTH1, 1:250, Abcam). Primary antibodies were incubated for 16 hr at 4°C, followed by detection by the following secondary antibodies: Alexa 568 donkey anti-rabbit or donkey anti-mouse (1:1000, Molecular Probes, Invitrogen) and Alexa 488 donkey anti-goat (1:1000, Molecular Probes, Invitrogen). Nuclei were counterstained with DAPI, and slides were mounted using Fluoromount (Calbiochem). Images were taken using either a Leica DM4000 upright microscope (Leica) or a Zeiss LSM 510 Meta Confocal Microscope. All images were taken and processed with equal settings.

Immunoblotting

Cells were collected and lysed in EBC buffer containing phosSTOP phosphatase inhibitor cocktail (Roche) and protease inhibitor cocktail (Sigma) and separated by a Novex NuPAGE 4-12% Bis-Tris protein gel (Invitrogen) and transferred to a Immobilon-FL PVDF membrane (Millipore). The membranes were blocked with 5% (wt/vol) dry milk in PBS-Tween-20 (0.5% vol/vol) and probed with primary antibodies against TfR (1:1000, Invitrogen), FTH1 (1:750, Abcam), FTL (1:1000, Abcam), FoxM1 (1:1000, Santa Cruz), STAT3 (1:1000, Cell Signaling), pSTAT3 y705 (1:1000, Cell Signaling), and β-actin (1:10,000, Sigma-Aldrich) as a loading control. For fluorescence-based detection, secondary antibodies were IRDye 800CW donkey anti-mouse IgG or donkey anti-rabbit IgG (1:20,000, LI-COR) and IRDye 600RD donkey anti-mouse IgG or donkey anti-rabbit IgG (1:20,000, LI-COR) and were applied for 1 hr at room

temperature. Membranes were developed using an Odyssey imaging system (LI-COR). For enhanced chemiluminescence, HRP mouse or rabbit secondary antibodies (1:2000, Cell Signaling) were detected with SuperSignal West Pico Chemiluminescent Substrate (Thermo Scientific). All Western blots were repeated at least 3 times.

Quantitative RT-PCR

Total cellular RNA was isolated with the RNeasy kit (Qiagen) and reverse-transcribed into cDNA using the qScript cDNA SuperMix (Quanta Biosciences). Real-time PCR was performed on an Applied Biosystems 7900HT cycler using SYBR-green Mastermix (SA Biosciences). Gene-specific primers as follows: *ACTB* (β-actin) forward 5'-AGAAAATCTGGCACCACACC-3' and reverse 5'-AGAGGCGTACAGGGATAGCA-3'; *GAPDH* forward 5'-GAAGGTGAAGGTCGGAGTC-3' and reverse 5'-GAAGATGGTGATGGGATTTC-3'; *FTH1* forward 5'-CTCCTACGTTTACCTGTCCATG-3' and reverse 5'-TTTCTCAGCATGTTCCCTCTC-3'; *FTL* forward 5'-AACCATGAGCTCCCAGATTC-3' and reverse 5'-CGGTCGAAATAGAAGCCCAG-3'; *SOX2* forward 5'-CACACTGCCCCTCTCAC-3' and reverse 5'-TCCATGCTGTTTCTTACTCTCC-3'.

Cell viability assay

For all experiments measuring cell viability, cells from dissociated xenografts were plated in triplicate in 96-well tissue culture treated plates at a density of 1000 cells per well. Relative ATP levels were measured at days 0, 1, 3, 5, and 7 days using CellTiter-Glo Luminescent Cell Viability Assay (Promega) according to manufacturer's instructions. Results are reported as relative fold change in ATP with each group internally normalized to its luminescence reading at day 0 (taken 6 hr post-plating).

Lentiviral Transduction

A non-targeting (NT) control shRNA sequence that is not expressed in the human transcriptome (SCH002; Sigma-Aldrich), served as a negative control for off-target effects. FTH1 shRNAs: NM_002032, 5 sequences: TRCN0000029429-33 and FTL shRNAs: NM_000146, 5 sequences: TRCN0000029434-38. To produce lentivirus, plasmids were co-transfected with packaging vectors psPAX2 and pCI-VSVG (Addgene) into 293FT cells using Lipofectamine 2000 (Invitrogen) or Fugene HD transfection reagent (Promega). For lentiviral transduction, cells were plated on geltrex-coated tissue culture treated plates and infected with a MOI ratio of ~ 5 viral particles per cell. Knockdown efficiency of FTH1 and FTL shRNA sequences were confirmed with qRT-PCR and western blot. FTH1 shRNA TRCN0000029433 (sequence: 5'-GCCGAATCTTCCTTCAGGATA-3') and FTL shRNA TRCN0000029434 (sequence: 5'-CTGGAGACTCACTTCCTAGAT-3') were validated as the best shRNAs to be used as each exhibited highest knockdown efficiency and no off-target effects.

FoxM1 Rescue Assay

CSCs were plated at a density of 1 x 10^5 cells/well in a 24-well plate already pre-coated with geltrex (Life Technologies). Following transduction with NT, FTH1, or FTL shRNAs, CSCs were transfected with FoxM1 overexpression or empty vector constructs. Cellular growth patterns were traced and calculated by taking the average of four measurements per well using the Incucyte Zoom (Essen BioScience).

Transferrin receptor biotinylation assay

Briefly, CSCs and non-CSCs from 4 different xenografts were cultured on geltrex-coated tissue culture plates incubated in identical medium conditions. 20 million cells were washed twice with PBS and pulse-labeled (30 min) with a cell-impermeable, cleavable biotinylation reagent (Sulfo-NHS-SS-Biotin, 0.3 mg/ml) to tag exposed primary amines of proteins in the cellular membrane of CSCs and non-CSCS, respectively. After quenching and cell lysis, biotinylated fraction of proteins was immunoprecipitated using affinity-purified using NeutrAvidin agarose resin. For

Western blot analysis, equal volumes (30 µl) of cytosolic (flow-through, biotin$^-$) and membrane (eluted, biotin$^+$) fractions were separated on 10% SDS-PAGE gel and probed for TfR (Invitrogen). ERK1/2 was used as a purity control (cytosolic marker) (Hamerlik et al., 2012).

Flow cytometric analysis and sorting

For TfR expression analysis, freshly dissociated xenografts (n ≥ 6) were incubated with TfR/CD71-PE antibody (BD Biosciences) for 1 hr at dilutions specified in the manufacturer's protocols. A BD FACSAria II sorter (BD Biosciences) was used to select, analyze, and sort TfR-positive and TfR-negative populations. Gating was determined using a LIVE/DEAD viability dye (Invitrogen) and an IgG2A Isotype control (BD Biosciences).

Microarray and microarray analysis

Microarray hybridization and processing were performed at the Case Western Reserve University Genomics Sequencing Core according to the manufacturer's protocol using the GeneTitan multichannel instrument (Affymetrix). Biotinylated cDNA fragments were generated from 500 ng of total RNA, and 180 ng of cDNA was hybridized onto the HuGene 2.1 PEG array (Affymetrix). The HuGene 2.1 array covers > 30,000 coding transcripts and 11,000 long internegic noncoding transcripts. Raw intensity values were normalized by robust multiarray average (RMA) analysis as previously described (Irizarry et al., 2003) using the Bioconductor oligo R package (Carvalho and Irizarry, 2010). Using the raw gene expression values, fold changes for each gene were calculated between each pair of non-targeting (NT) and FTH1 or FTL shRNA condition. As an input for further analysis, we used only genes that were consistently decreased by 2-fold, with a p value < 0.05. Genes that met this threshold were analyzed using Ingenuity Pathway Analysis (IPA, Ingenuity Systems) with the threshold of a more than 2-fold expression difference. For calculations of mRNA levels for *FOXM1* and downstream targets, values were first normalized by RMA analysis followed by fold changes for

each gene calculated by comparing expression from non-targeting (NT) shRNA to either FTH1 or FTL shRNA condition within each specimen.

Chromatin Immunoprecipitation

FoxM1 chromatin immunoprecipitation experiments were performed using 5 µg of FoxM1 antibody (GeneTeX) per IP as described previously (Mack et al., 2014). Predicted FoxM1 binding sites and negative control regions (up- or down- stream) were identified by mining the ENCODE database for published FoxM1 ChIP-seq profiles. FoxM1 occupancy was quantified relative to input and normalized against a matched negative control (upstream or downstream of the FoxM1 predicted binding site). FoxM1 enrichment was quantified using SYBR green real-time PCR (Invitrogen), and performed in three technical replicates. Error bars are graphed as percent error. Positive and negative control primers are listed below for positive controls: *PLK1* forward 5'-CCGTGTCAATCAGGTTTTCC-3' and reverse 5'-GCTGGGAACGTTACAAAAGC-3', *AURKB* forward 5'-CCAACGGACCCTCTGATCTA-3' and reverse 5'-GGGAGAGTAGCAGTGCCTTG-3', *CDK1* forward 5'- AAAGAAGAACGGAGCGAACA-3' and reverse 5'-GCTAGAGCGCGAAAGAAAGA-3', *CENPF* forward 5'-CACCTCCAGTAGAGGGCTTG-3' and reverse 5'-TACCTCCACGCCTATTGGTC-3'. Primers for negative controls: *PLK1* forward 5'-TGTCTCCCCTTAGAGGCTGA-3' and reverse 5'-GACAGCTGTGGTCCAAGTGA-3', *AURKB* forward 5'-AGTGCAGTGGTGTGATCTCG-3' and reverse 5'-ATTAGCTGGGAGTGGTGGTG-3', *CDK1* forward 5'-CTCCTGCTCAGATCCTTTGG-3' and reverse 5'-GAGTGGGCCTTCCATACAGA-3', *CENPF* forward 5'-CTTGCAAGGAGCCTAGATCG-3' and reverse 5'-ATTCCCAGACACAAGCAACC-3'.

Retrospective analysis of *TFRC*, *FTH1*, *FTL and FOXM1* gene expression in human gliomas

Correlations between glioma grade, patient survival and gene expression were determined through analysis of TCGA, Sun, Nutt, Freije, and Phillips brain data sets, which are available

through Oncomine (Compendia Biosciences, http://www.oncomine.org/). High and low groups were defined as above and below the mean, respectively. For analysis with high, medium and low groups, high was defined as greater than 1 s.d. above the mean, low as greater than 1 s.d. below the mean and medium as within 1 s.d. of the mean. The National Cancer Institute's REMBRANDT (https://caintegrator.nci.nih.gove/rembrandt/) was also evaluated for correlations between glioma patient survival and gene expression with up- or downregulation being defined as a twofold change relative to mean values.

Statistical analysis and sample sizes

All grouped data are presented as mean ± S.E.M. Difference between groups was assessed by ANOVA with a Bonferroni's post hoc test, Student's *t*-test, or log-rank (Mantel-Cox), where appropriate, using GraphPad Prism software. For survival analysis, Kaplan-Meier curves were generated and log-rank analysis were also performed using Prism software. We used short-term passage cells (less than 5 passages both in terms of xenograft passage and passage in culture). Typical proportions of CSCs isolated from fresh GBM specimens or xenograft were usually 10% or less than the dissociated tumor bulk. We observed consistent results across all specimens used in this manuscript. For mouse experiments, sample sizes were calculated using the formula $n = 1 + 2C\,(\sigma/d)^2$, where n = number of animals per arm, $C = 7.85$ (significance level of 5% with a power of 80%), σ = s.d and d = difference to be detected. For other experiments, no statistical methods were used to predetermine sample sizes, but our sample sizes are similar to those in our previous publications.

Supplemental References

Carvalho, B.S., and Irizarry, R.A. (2010). A framework for oligonucleotide microarray preprocessing. Bioinforma. Oxf. Engl. *26*, 2363–2367.

Das, N.K., Biswas, S., Solanki, S., and Mukhopadhyay, C.K. (2009). Leishmania donovani depletes labile iron pool to exploit iron uptake capacity of macrophage for its intracellular growth. Cell. Microbiol. *11*, 83–94.

Hamerlik, P., Lathia, J.D., Rasmussen, R., Wu, Q., Bartkova, J., Lee, M., Moudry, P., Bartek, J., Fischer, W., Lukas, J., et al. (2012). Autocrine VEGF-VEGFR2-Neuropilin-1 signaling promotes glioma stem-like cell viability and tumor growth. J. Exp. Med. *209*, 507–520.

Hu, B.-Y., Du, Z.-W., and Zhang, S.-C. (2009). Differentiation of human oligodendrocytes from pluripotent stem cells. Nat. Protoc. *4*, 1614–1622.

Irizarry, R.A., Hobbs, B., Collin, F., Beazer-Barclay, Y.D., Antonellis, K.J., Scherf, U., and Speed, T.P. (2003). Exploration, normalization, and summaries of high density oligonucleotide array probe level data. Biostat. Oxf. Engl. *4*, 249–264.

Langmead, B., Trapnell, C., Pop, M., and Salzberg, S.L. (2009). Ultrafast and memory-efficient alignment of short DNA sequences to the human genome. Genome Biol. *10*, R25..

Li, H., Handsaker, B., Wysoker, A., Fennell, T., Ruan, J., Homer, N., Marth, G., Abecasis, G., Durbin, R., and 1000 Genome Project Data Processing Subgroup (2009). The Sequence Alignment/Map format and SAMtools. Bioinforma. Oxf. Engl. *25*, 2078–2079.

Mack, S.C., Witt, H., Piro, R.M., Gu, L., Zuyderduyn, S., Stütz, A.M., Wang, X., Gallo, M., Garzia, L., Zayne, K., et al. (2014). Epigenomic alterations define lethal CIMP-positive ependymomas of infancy. Nature *506*, 445–450.

Ramsköld, D., Wang, E.T., Burge, C.B., and Sandberg, R. (2009). An abundance of ubiquitously expressed genes revealed by tissue transcriptome sequence data. Plos Comput. Biol. *5*, e1000598.

Sarkar, J., Seshadri, V., Tripoulas, N.A., Ketterer, M.E., and Fox, P.L. (2003). Role of ceruloplasmin in macrophage iron efflux during hypoxia. J. Biol. Chem. *278*, 44018–44024.

Stoppini, L., Buchs, P.-A., and Muller, D. (1991). A simple method for organotypic cultures of nervous tissue. J. Neurosci. Methods *37*, 173–182.

Suvà, M.L., Rheinbay, E., Gillespie, S.M., Patel, A.P., Wakimoto, H., Rabkin, S.D., Riggi, N., Chi, A.S., Cahill, D.P., Nahed, B.V., et al. (2014). Reconstructing and reprogramming the tumor-propagating potential of glioblastoma stem-like cells. Cell *157*, 580–594.

Trapnell, C., Pachter, L., and Salzberg, S.L. (2009). TopHat: discovering splice junctions with RNA-Seq. Bioinforma. Oxf. Engl. *25*, 1105–1111.

Trapnell, C., Williams, B.A., Pertea, G., Mortazavi, A., Kwan, G., van Baren, M.J., Salzberg, S.L., Wold, B.J., and Pachter, L. (2010). Transcript assembly and quantification by RNA-Seq

reveals unannotated transcripts and isoform switching during cell differentiation. Nat. Biotechnol. *28*, 511–515.

Zhang, Y., Liu, T., Meyer, C.A., Eeckhoute, J., Johnson, D.S., Bernstein, B.E., Nusbaum, C., Myers, R.M., Brown, M., Li, W., et al. (2008). Model-based analysis of ChIP-Seq (MACS). Genome Biol. *9*, R137.